



Impact of specimen preparation method on photovoltaic backsheet degradation during accelerated aging test

Ji Xia¹  | Yi Liu² | Hongjie Hu¹ | Xiaogang Zhu² | Hao Lv¹ | Nancy H. Phillips³ | Kaushik Roy Choudhury³ | William J. Gambogi³ | Marisol Rodriguez³ | Ethan S. Simon³ | Michael Kempe⁴  | Joshua Morse⁴

¹DuPont (China) Research & Development and Management Co. LTD., Shanghai, China

²National Center of Supervision and Inspection on Solar Photovoltaic Product Quality (CPVT), Wuxi, China

³DuPont Company, Wilmington, Delaware, USA

⁴National Renewable Energy Laboratory (NREL), Golden, Colorado, USA

Correspondence

Hongjie Hu, DuPont (China) Research & Development and Management Co. LTD., No. 600, Cailun Rd, Zhangjiang Hi-Tech Park, Shanghai 201203, China.
Email: Hongjie.Hu@dupont.com

Abstract

In this study, we highlight some important factors in the specimen preparation methods for evaluating photovoltaic backsheet properties after accelerated aging. Two different sequences are considered: Method (I) cut-then-age: cut into 1-cm wide strips and then expose to stress, and Method (II) age-then-cut: expose a larger sheet to stress and then cut into 1-cm widths for mechanical property measurements. We also compare the effect of three cutting methods, (a) tensile specimen punch, (b) paper cutter, and (c) fresh razor blade. Several commercial backsheets were evaluated, with stress exposures including (a) pressure cooker test (PCT), (b) dry ultraviolet (UV) radiation exposure, and (c) UV combined damp heat tests. Fourier transform infrared spectrometer (FTIR) and intrinsic viscosity (IV) were used to analyze the materials on unstressed materials and samples exposed to PCT. The results show that both the cutting method and the time of cutting have an impact on the backsheet mechanical properties. Under UV exposure, Method II, age-then-cut, generally resulted in a higher average value, with more variation than Method I; however, if the side strips from Method II were excluded, the variation dropped to the same level. This is because the specimens at the sides of the sheet get additional damage from UV light from the exposed sides of the sample. In contrast to UV exposure, PCT specimens prepared by Method II result in lower average values and higher variability. This is attributed to embrittlement through the bulk of the sample where the cutting of embrittled specimens appears to result in more edge defects which can then initiate a break at smaller strains. The data suggest that for UV exposures, the specimens should be cut after aging and the exposed side specimens discarded, and that for PCT exposures, the specimens should be cut before the exposure.

KEYWORDS

accelerated aging test, cutting, embrittlement, photovoltaic backsheet, sample preparation, tensile testing

This is an open access article under the terms of the Creative Commons Attribution License, which permits use, distribution and reproduction in any medium, provided the original work is properly cited.

© 2022 The Authors. *Energy Science & Engineering* published by the Society of Chemical Industry and John Wiley & Sons Ltd.

1 | INTRODUCTION

With photovoltaic (PV) technology being competitive with traditional energy sources in a wide variety of markets, global PV installations have grown rapidly, and are expected to continue at a double-digit growth rate over the next decade. Projections for 2021 are that 158 GW of new PV will be installed globally, an increase of 34% over the installation rate in 2020. However, analysts expect the PV market to be a “wild ride.”¹

A PV backsheet, as one of the crucial parts of PV module, must possess sufficient mechanical properties, electrical insulation performance, and moisture barrier properties to protect the solar cell and maintain electrical safety for more than 25 years in a diverse set of environments. Hence, more and more attention has been paid to the quality, reliability, and durability of backsheets.

In recent years, PV backsheet failures in the field have increasingly been observed and attracted wide attention of backsheet quality concerns to the PV. In particular, cracking of polyamide (PA) and polyvinylidene fluoride (PVDF) based backsheets, and other failures, have been observed.^{2–4} Although these backsheets passed the testing required by IEC 61730 ed. 2nd and 3rd party certification, they were not durable in the application. Consequently, standards are in development which emphasize increased performance requirements for material assessment, including after environmental stress exposures. These concerns are addressed in part in an IEC standard for backsheets (IEC TS 62788-2)⁵ and many other national and industrial backsheet related standards⁶ which have been published in the last 5 years. The new edition of IEC 61730 (ed. 3) will include new minimum requirements defined in IEC 62788-2-1, the backsheet safety qualification standard. Among these new requirements, are tests utilizing retention of elongation to break after aging.

An important step forward has been the implementation of accelerated aging tests specified in these standards. To mimic backsheet outdoor performance, various accelerated aging methods have been used.^{7–11} Single stress tests are generally performed under various combinations of exposure to damp heat (DH), ultraviolet (UV), and thermal cycling (TC). Sequential tests^{12,13} are recommended by some 3rd parties, such as researchers at the National Renewable Energy Laboratory (NREL)^{14–16} and Photovoltaic Evolution Labs (PVEL),^{17,18} which can better simulate field conditions and observed failure modes. A comprehensive aging test, combining UV, DH, and TC together,¹⁹ was also developed at DuPont. IEC TS 63209-1²⁰ includes a set of extended testing for modules,

and IEC TS 63209-2²¹ includes extended testing for components.

Inherent to these backsheet durability evaluations is the measurement of tensile properties before and after accelerated stress exposures. The general method is established in the PV industry, but limited studies²² have investigated the effect of backsheet specimen preparation method on the measured values. The previous study considered the effect of cutting method, comparing fresh razor blade (specimens all cut in one laboratory) and a variety of paper cutters (from several laboratories).

In this study, we examine how sample preparation methods can influence measured loss of tensile properties of backsheets after accelerated aging. This includes evaluation of the sequence of stress and cutting, and the method of cutting. The materials evaluated included several different commercial backsheets with PET cores and the known bad AAA PA based backsheet. The sequence of cutting and stress exposure was evaluated using either Method I (cut-then-age) or Method II (age-then-cut). Four steady state environmental stress exposures were used, including pressure cooker test (PCT), dry UV^{23–25} and ultraviolet metal halide (UVMH)²⁶ with DH. Specimens were characterized by retention of tensile properties, Fourier transform infrared spectrometer (FTIR) and intrinsic viscosity (IV). We compare the effect of cutting methods: (a) tensile specimen punch, (b) paper cutter, and (c) fresh razor blade, on unstressed materials and samples exposed to PCT using both Methods I and II.

2 | MATERIALS AND METHODS

2.1 | Backsheets

Eight different commercial backsheets were used in this study. The backsheet structures, aging tests and characterization methods were listed in Table 1.

2.2 | Cutting methods

Three cutting methods used in this study as shown in Figure 1.

Samples exposed in UV Metal Halide chamber were cut by razor blade (Figure 1C), and those exposed to UV Xenon chamber were cut with a tensile specimen punch (Figure 1A). PCT specimens were cut using all three methods. For the Method I sequence, the backsheet was cut into 1 cm strips and then put into the chamber for

TABLE 1 Backsheet used in this study

Abbr.	Structure (out layer/ core layer/inner layer)	Aging tests	Characterization methods
D1	PVDF/PET/PVDF	UVX, UVMH, PCT	Mechanical properties, Intrinsic viscosity
D2	PVDF/PET/Coating	UVX, UVMH, PCT	Mechanical properties, Intrinsic viscosity, FTIR
T1	PVF/PET/PVF	UVX, UVMH, PCT	Mechanical properties, Intrinsic viscosity.
T2	PVF/PET/PE	UVMH	Mechanical properties
A1	PA/PA/PA	UVMH	Mechanical properties
P1	PET/PET/PE	UVMH, PCT	Mechanical properties
T3	PVF/PET/PE	PCT	Mechanical properties, microscope
T4	PVF/PET/PE	PCT	Mechanical properties

Abbreviations: FTIR, Fourier transform infrared spectrometer; PA, polyamide; PCT, pressure cooker test; PVDF, polyvinylidene fluoride; UVMH, ultraviolet metal halide; UVX, ultraviolet Xenon.



FIGURE 1 Cutting method photos. (A) Tensile specimen punch (JDC precision sample cutter) (B) paper cutter, and (C) fresh razor blade

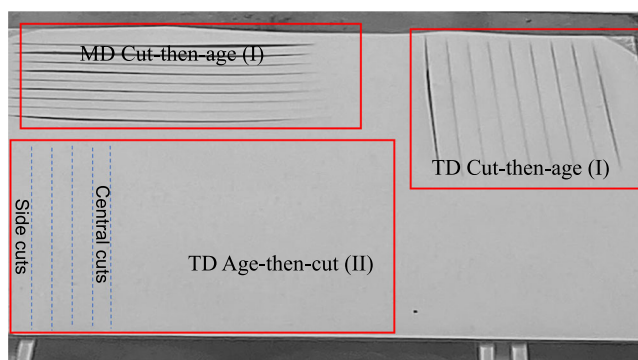


FIGURE 2 Schematic of specimen preparation used for ultraviolet metal halide exposures. Cut using a razor blade: cut-then-age (Method I), and age-then-cut (Method II)

aging. For the Method II sequence, a larger sheet was put into the environmental chamber and then cut into strips after the exposure was completed. To aid in specimen tracking, specimens were frequently cut but not separated before environmental exposure as shown in Figure 2. In this study, “specimen” refers to a 1 cm strip used for mechanical properties measurement; “sample” refers to the material exposed in the environmental chamber.

2.3 | Equipment

2.3.1 | Aging chamber and test conditions

Ultraviolet Xenon (UVX) aging test

Exposures were conducted in Atlas Ci4000 weatherometers with UV Xenon lamp (UVX) and daylight filter (TAP-S) combination with a Right Light inner filter. This produces an irradiation spectrum closely matching sunlight. The A3 condition of IEC TS 62788-7-2 (2017) is used in this UVX aging test, which (A3 condition) specifies UV exposure intensity of $0.8 \text{ W/m}^2/\text{nm}@340 \text{ nm}$, chamber temperature of 65°C and black panel temperature 90°C for 1000 h and 2000 h, respectively, on the airside with an expected specimen temperature of $70\text{--}75^\circ\text{C}$ for a white backsheet sample due to absorption of incident light. The UV dose is 80 and 160 kWh/m^2 .

UVMH plus DH aging test

As a combined weathering test, UVMH exposure was applied together with DH conditions to characterize material degradation. Exposures were conducted in Xianghao GRO-SUV5000TH UV DH aging test chamber

equipped with a metal halide lamp with a light filter having a cutoff wavelength of 280 nm. Two different steady state exposure conditions were used for comparison: UVMH + DH (65°C/65% RH) and UVMH + DH (85°C/85% RH), both with H2 filter. Temperature was controlled by thermocouple on the sample; therefore, the listed temperatures are sample temperatures. UV intensity was controlled at 160–180 W/m² @280–400 nm for a total dose of 100 or 150 kWh/m², the expose time is about 588 and 882 h, respectively.

PCT

PCT exposures were conducted in a HIRAYAMA PC-304/422R8 HAST chamber. PCT testing increases the absorption level of moisture in materials. This is accomplished by applying pressure under set conditions of temperature and humidity continuously. A standard test condition of PCT is 121°C, 100% RH and under 2 atm for 48 h was used.

2.4 | Mechanical properties

Mechanical properties are critical indicators of material aging behavior, with backsheets maintaining a high elongation at break (ϵ_b) expected to demonstrate long-term durability and stability of solar modules in field. In this study, tensile tests according to IEC TS 62788-2 or ASTM D882 were carried out to measure the strain at break, ϵ_b . The tensile tests were carried out with either an Instron 5967 (High Wycombe) tensile testing machine at 23°C, and a cross head speed of 100 mm/min; or an Instron 5500 R, with cross head speed of 50 mm/min.

2.5 | Analytical characterization

Attenuated total refraction (ATR-FTIR) and intrinsic viscosity were used to characterize the backsheets. FTIR (iN10, Thermofisher) was used to investigate changes of chemical structure. Meanwhile, intrinsic viscosity in Phenol-1,1,2,2-tetrachloroethane mixture 50:50% (V/V) was used to characterize the molecular weight and its distribution of these samples, microscope (Nikon ME600L) was used to investigate the edge morphology.

3 | RESULTS AND DISCUSSION

3.1 | UVX

3.1.1 | Mechanical properties after UVX

Elongation at break (ϵ_b) of three backsheets, measured for five specimens taken from the side (#1) to center (#5) of the backsheet sample, were measured after 1000 h and 2000 h UVX, with samples cut using both the Method I and Method II sequences. Figures 3 and 4 show the data for each specimen, with some notable differences. Specimen #1 of the Method II (age-then-cut), where the edge was exposed to UV, is significantly lower than the remainder of the specimens for each of the backsheets. Removing data for these specimens increases the average and reduces the standard deviation, which were shown in Table 2. The specimens prepared using Method I (cut-then-age) has a higher consistency but a lower average. This is expected if both edges of all specimens were exposed to UV. In Tables 2 and 3, the ϵ_b of specimens by Method I after UVX 2000hrs show more

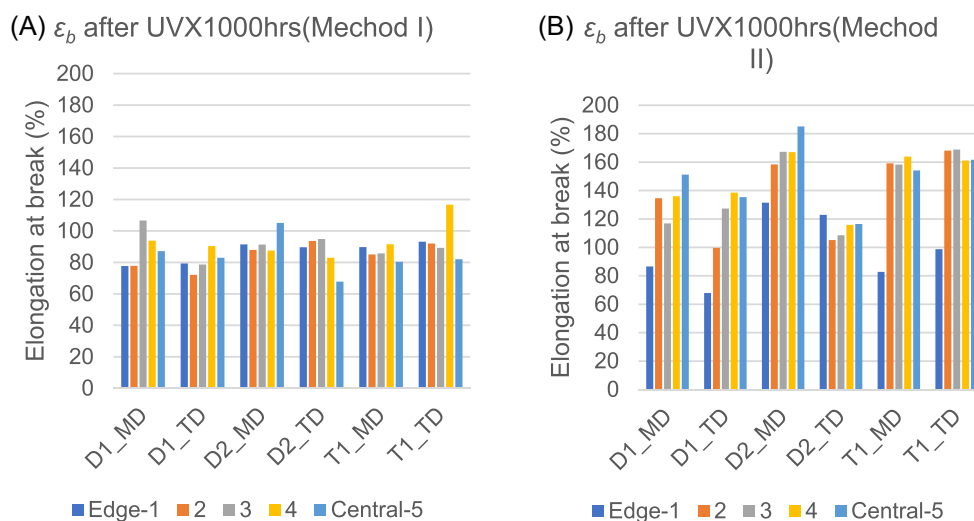


FIGURE 3 Percent elongation at break (ϵ_b) after UVX 1000 h. Pulled at 100 mm/min. The “Side-1” specimen was cut from the side of a sheet after exposure. (A) Cut-then-aged. (B) Aged-then-cut

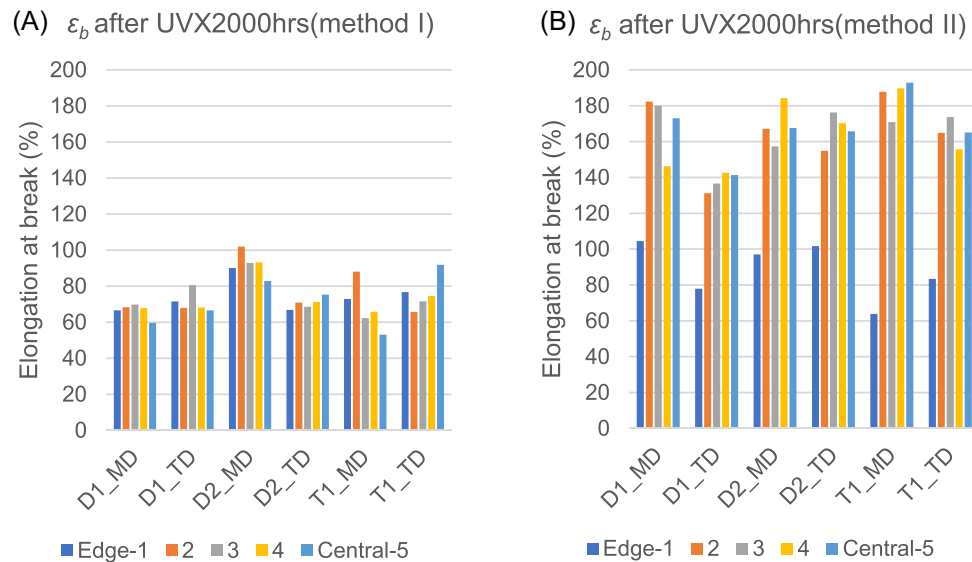


FIGURE 4 Percent elongation at break (ϵ_b) after UVX2000 h. Pulled at 100 mm/min. Method I: Cut-then-aged. Method II: Aged-then-cut

TABLE 2 Percent elongation at break (ϵ_b) after UVX 1000 h

	Method I cut-then-age	Method II age-then-cut (including side specimen)	Method II age-then-cut (excluding side specimen)
D1_MD	89 ± 12	125 ± 25	135 ± 14
D1_TD	81 ± 7	114 ± 30	125 ± 18
D2_MD	93 ± 7	162 ± 20	169 ± 11
D2_TD	86 ± 11	114 ± 7	112 ± 6
T1_MD	86 ± 4	144 ± 34	159 ± 4
T1_TD	95 ± 13	152 ± 30	165 ± 4

Note: Pulled at 100 mm/min. Mean and standard deviation.

TABLE 3 Percent elongation at break (ϵ_b) after UVX2000 h

	Method I cut-then-age	Method II age-then-cut (including side specimen)	Method II age-then-cut (excluding side specimen)
D1_MD	66 ± 4	157 ± 33	170 ± 17
D1_TD	71 ± 6	126 ± 27	138 ± 5
D2_MD	92 ± 7	155 ± 34	169 ± 11
D2_TD	71 ± 3	154 ± 30	167 ± 9
T1_MD	68 ± 13	161 ± 55	185 ± 10
T1_TD	76 ± 10	149 ± 37	165 ± 7

Note: Pulled at 100 mm/min. Mean and standard deviation.

repeatable data, with the standard deviation of all 6 specimens ranging from 3% to 13%. Specimens tested by Method II range from 27% to 55%, but if data from the side strip is removed, the average increased and the standard deviation dropped to a range of 5% to 17%, consistent with Method I. This shows an edge effect

indicating that severity of aging is quite different for different parts of the specimen, with the edge more degraded.

Comparing the mean ϵ_b of these three backsheets specimens cut and exposed by Methods I and II, ϵ_b from Method I is lower along both machine direction (MD)

and transverse direction (TD), and can likely be ascribed to more severe degradation on the edges of each test specimen in Method I. For example, T1_MD ϵ_b by Method I after UVX2000hrs is 68%, while that by Method II is 161%. In Method I, the data indicate more degradation.

The UVX test data indicates that: (a) Lower standard deviation is observed with Method I across all backsheet types and for both specimen orientations, (b) Specimens prepared by Method I show more severe degradation for the side test specimens, and (c) ϵ_b of the side specimens by Method II is well below the mean value, which shows an edge effect of the UV exposures which has previously been demonstrated.⁵ This is consistent with the Method I measurements, where each specimen had two side specimens with edges exposed to UV, and supports the guidance provided by IEC TS 62788-2 which excludes the use of the side cut specimens after UV exposure.

3.1.2 | FTIR

Peak height ratio of cross section Micro-ATR FTIR spectrum of core layer PET was used to characterize material degradation levels and compare specimens.^{27,28} Specimens are epoxy cured and then polished to obtain the cross section of the core layer PET. And then Micro-ATR FTIR method has been utilized to characterize degradation levels of different specimens, with the spectra shown in Figure 5. The carbonyl group is destroyed during photodegradation, while the benzene ring is relatively stable, so the ratio of carbonyl peak to the aromatic to C-H peak is useful to characterize the aging performance, summarized in Table 4. After UVX2000, the ratio of C=O to C-H for the side specimen D2-1 is 8.31 compared to 8.68 for a central specimen (D2-5). The results show that more degradation occurred in D2-1, consistent with the ϵ_b results (Figures 3 and 4).

3.2 | UVMH

3.2.1 | Mechanical properties after UVMH

The average ϵ_b values of the backsheets after UV + DH (65°C/65% RH) 100 and 150 kWh/m² using the two sequences are shown in Figure 6. For all except the most degraded specimens, Method II values are higher than for Method I, indicating² more degradation occurred in all specimens by Method I (cut-then-age). This is consistent with the results from UV A3 exposure indicating that the combination of slightly lower

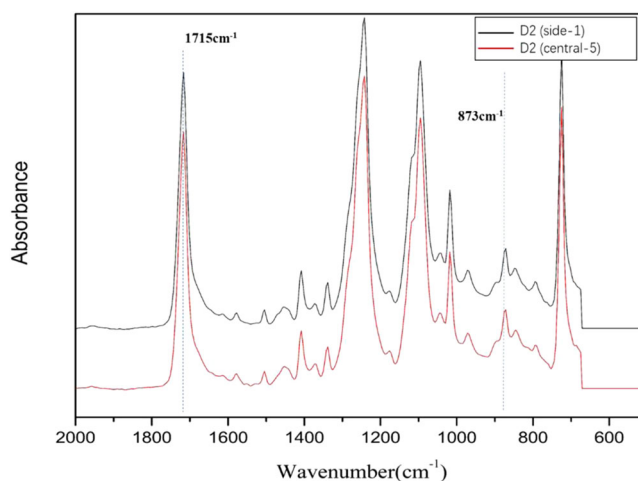


FIGURE 5 Fouriertransform infrared spectromete of cross section PET of side-1 and central-5 of D2 by Method II after UVX2000

TABLE 4 Ratio of carbonyl to C-H benzene ring after UVX2000

Method II	C=O	Ar C-H	Ratio
D2-(side-1)	0.432	0.052	8.31
D2-(central-5)	0.434	0.05	8.68

temperature, but higher humidity did not significantly change the degradation characteristics.

UV + 85°C/85% RH aging test is of interest as it combines the DH condition of 85°C/85% RH with UV exposure and may shorten the time to achieve failure, achieving greater degradation than in UV + 65°C/65% RH, Figure 6. However, care should be taken to demonstrate that the degradation mechanism is still relevant. Again, for all except the most degraded specimens (where valid measurements were not obtained), Method II values are higher than for Method I, indicating more degradation occurred in the specimens with two exposed edges for both the MD and TD specimens.

3.3 | PCT

3.3.1 | Mechanical properties after PCT

PCT, as a harsh aging test that leads to unrealistic failure modes rarely seen in the field, has been widely used in laboratories for its high efficiency. Our work mainly studies the influence of different sample preparation methods on laboratory test results. Thus, PCT is worth to be discussed here.

Four of the backsheets were subjected to PCT with specimens prepared using a precision tensile punch and both sequences of Methods I and II. The ϵ_b specimen values are shown in Figure 7. Most notable is the

difference in the average values. The T1 and D1 backsheets using Method II show considerably lower ϵ_b values than by Method I, while the P1 and D2 averages were similar between the two methods.

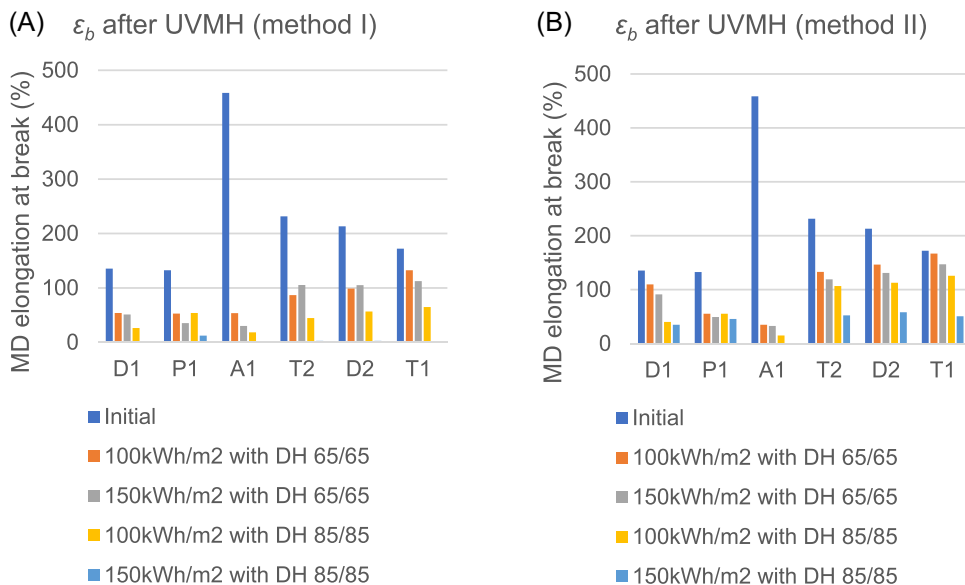


FIGURE 6 Elongation at break of machine direction (ϵ_b) of backsheet specimens. (A) Cut-then-aged. (B) Aged-then-cut

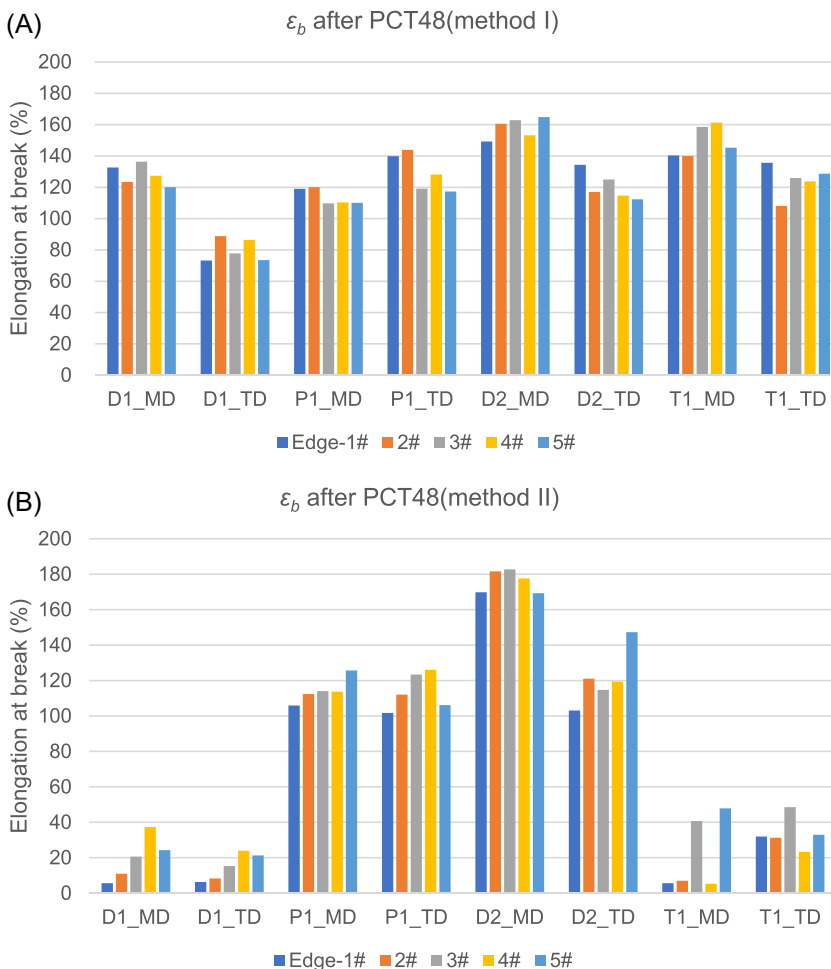


FIGURE 7 Elongation at break (ϵ_b) after PCT48 (48 h, 121°C, 2 atm). Samples cut using the tensile specimen punch. (A) Cut-then-aged. (B) Aged-then-cut

(Note that the D2_MD values are ~15% higher in Method II, which was surprising; without further work, we are attributing this to reproducibility issues). The standard deviation of the Method I specimens was low for all the materials, with more variance seen for the Method II specimens. For D1_MD, the deviation of specimens by Method I is 6.6%, while that by Method II is up to 12.3%. These results are consistent with a model where the bulk is degrading through hydrolysis, initiated at micro-point defect sites; if a cut is made at a defect point, the specimen is more likely to break; thus the average and standard deviation are impacted. In contrast to the results with UV exposures, the results suggest that for bulk degradation mechanisms such as hydrolysis, Method I is preferred.

The degradation variance of different cut locations of specimens was tested by both Methods I and II. For Method I, there is not a significant difference between the five specimens from the side to the center. For Method II (age-then-cut), the data do not show an edge effect, except possibly for D1 MD/TD specimens. But here, the samples are extremely degraded and the effect appears to be much more than just an edge effect extending 3 or 4 mm into the sample. Most likely, this is related to random variation or residual stress.

3.3.2 | Intrinsic viscosity after PCT

Intrinsic viscosity (η) is a measure of a solute's contribution to the viscosity η of a solution. Intrinsic viscosity is defined as:

$$[\eta] = \lim_{\phi \rightarrow 0} \frac{\eta - \eta_0}{\eta_0 \phi}$$

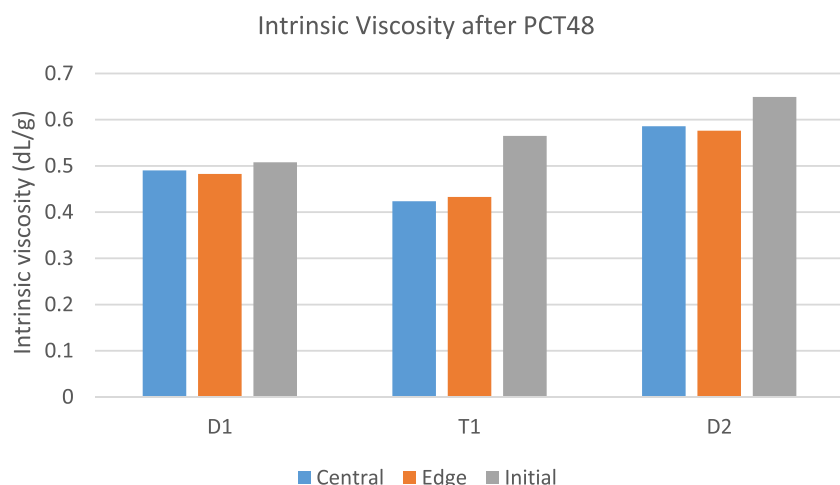


FIGURE 8 Intrinsic viscosity after PCT48 by Method II

The intrinsic viscosity value of PET-based backsheets are correlated to the molecular weight. Specimens tested after PCT in Method II were selected for viscosity measurement and the results were shown in Figure 8. The blue bar and the red bar show intrinsic viscosity of the central area and the side area (the edge ~1 mm of the side specimens) after 48 h of the PCT test (PCT48), while gray column represents initial data before aging. The results indicated that there is no meaningful difference in the intrinsic viscosity between the side specimen and the central specimen after PCT48. This observation is also consistent with the ε_b data in Figure 7.

3.3.3 | Effect of cutting method

In this set of experiments, two PET-core backsheets were cut using three different cutting methods: (a) tensile specimen punch, (b) paper cutter, and (c) fresh razor blade. Samples were exposed to PCT using both Method I (cut-then-age) and Method II (age-then-cut). Figure 9 shows the edge micrographs after different cutting methods. The edge graphs from punch and paper cutter are similar, while that from razor blade are quite different, and this might be caused by the difference of cutting force direction between razor blade and the other two cutting methods.

Figure 10 shows the results for unaged specimens. Contrary to what was observed in an initial study,²² little difference was observed between the razor and paper cutter methods. The punch method gave the same results for Backsheet T3, and higher for backsheet T4.

Figure 11 shows the results for aged specimens. Here, the cutting method showed a significant impact.

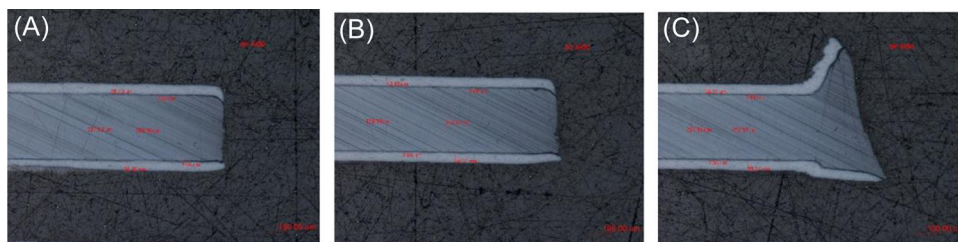


FIGURE 9 Edge micrographs after different cutting methods. (A) Tensile specimen punch (B) paper cutter, and (C) fresh razor blade

FIGURE 10 ϵ_b of unaged backsheet specimens using different cutting methods

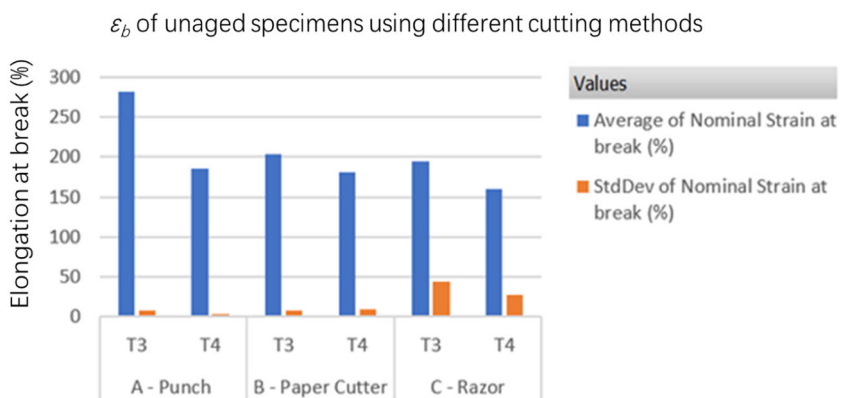
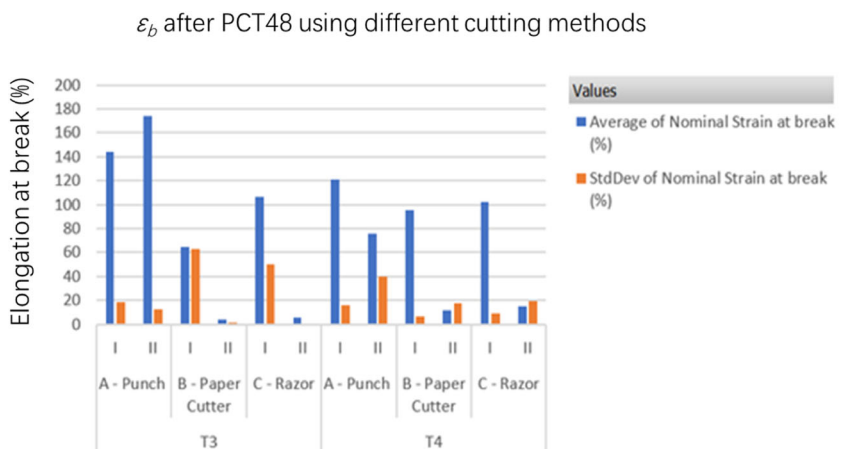


FIGURE 11 ϵ_b of pressure cooker test aged backsheet specimens using Method I or Method II



For Backsheet T3, the punch values were the same as specimens which were cut-then-aged (Method I) as for specimens which were aged-then-cut (Method II). However, for the paper cutter and razor cut specimens, cutting after aging (Method II) resulted in very low values, while the pre-cut specimens were much higher. A similar effect was observed for Backsheet T4. Note also the large standard deviation for most of the values with averages between 10% and 80%. This demonstrates the difficulty of getting a reproducible cutting method for embrittled PET materials.

4 | CONCLUSIONS

In this study, the influence of two different stress/cut sequences, cut-then-age (Method I) and age-then-cut (Method II), and the method of cutting on backsheet degradation behavior were investigated. The mechanical test results suggest that specimens prepared with the sequence of Method I show lower ϵ_b than that by Method II, independent of backsheet type, specimen direction, or environmental condition when exposed to UV light. This is because when the samples are cut before UV exposure

the edges of the PET layer are directly exposed to UV light and degraded more than the bulk. This fits a model where the embrittled material is more susceptible to creation of edge defects during the cut, which then are then more likely to initiate a break during the tensile test. When exposed to PCT tests, the embrittlement of the PET layer occurs uniformly throughout the bulk of the film. When the cut is made after exposure, the highly embrittled PET is more likely suffer edge defects during the cutting process, resulting in a break initiated at a lower ε_b . The results clearly indicate that the preparation method impacts the mechanical property results and that the type of degradation has a significant effect on the effect of the cutting timing.

Cutting method can also cause significant differences of ε_b . In this study, a tensile specimen punch produced higher ε_b values than the specimen by the other two cutting methods. The result depends not only on the material type, aging conditions and specimen cutting methods, but also can be affected by cutting implement and a particular individual, especially for brittle materials. Thus, it is possible that conflict conclusions can be drawn from else research.²²

For the UV exposures, edge effects caused more variability for the specimens cut after exposure, which was reduced when the side specimens were removed from the average. These results suggest that for UV exposures of backsheets containing PET, the specimens should not be cut before aging, as the edges will be artificially degraded and lower the results. Additionally, when UV exposed samples are cut, the side specimens should be discarded.

In summary, these data suggest that for exposures using only heat or heat/humidity, more relevant and consistent results are obtained by cutting before exposure, while for UV aging, cutting should be done after exposure, with the edge-exposed material discarded.

ACKNOWLEDGMENTS

The authors would like to thank Dr. Michael Thomas Demko for his support during all the rounds of discussion and review. We are also very grateful to DuPont China Analytical Center and CPVT Test Platform for their support in testing and characterization work. This study was supported by the Guided local science and technology development projects from the central government (2021FRD05006), and National key research and development program (2020YFB1506505).

ORCID

Ji Xia  <http://orcid.org/0000-0003-2320-9854>

Michael Kempe  <http://orcid.org/0000-0003-3312-0482>

REFERENCES

1. Mark H. *New PV Installations to Reach 158 GW Next Year, Says IHS Markit*; 2020. <https://www.pv-magazine.com/2020/12/18/new-pv-installations-to-reach-158-gw-next-year-says-ihs-markit/>
2. Eder GC, Voronko Y, Oreski G, et al. Error analysis of aged modules with cracked polyamide backsheets. *Sol Energy Mater Sol Cells*. 2019;203:110194.
3. Gambogi WJ, Kopchick J, Felder T. *Sequential and Weathering Module Testing and Comparison to Fielded Modules*. NREL Photovoltaic Reliability Workshop; 2015.
4. Han H, Xia J, Hu H, et al. Aging behavior and degradation of different backsheets used in the field under various climates in China. *Sol Energy Mater Sol Cells*. 2021;225:111023.
5. IEC TS 62788-2. Revision 1.0. *Measurement Procedures for Materials Used in Photovoltaic Modules—Part 2: Polymeric Materials—Frontsheets and backsheets*. International Electrotechnical Commission; 2017:1-88.
6. GB/T 31034-2014. *Insulating Back Sheet for Crystalline Silicon Terrestrial Photovoltaic (PV) Modules*. The Chinese National Standard; 2014:1-14.
7. Kim N, Kang H, Hwang KJ, et al. Study on the degradation of different types of backsheets used in PV module under accelerated conditions. *Sol Energy Mater Sol Cells*. 2014;120:543-548.
8. Knausz M, Oreski G, Eder GC, et al. Degradation of photovoltaic backsheets: comparison of the aging induced changes on module and component level. *J Appl Polym Sci*. 2015;132(24):n/a.
9. Zhang JW, Cao DK, Cui YC, Wang F, Putson C, Song C. Influence of potential induced degradation phenomena on electrical insulating backsheet in photovoltaic modules. *J Clean Prod*. 2019;208:333-339.
10. Fairbrother A, Julien S, Wan K-T, et al. Degradation analysis of field-exposed photovoltaic modules with non-fluoropolymer-based backsheets. In: Dhere NG, Sakurai K, Kempe MD, eds. *Reliability of Photovoltaic Cells, Modules, Components, and Systems X*. International Society for Optics and Photonics; 2017.
11. Bruckman L, Wang Y, French R, et al. *Backsheets: Correlation of Long-Term Field Reliability with Accelerated Laboratory Testing (No. DOE-UL-0007143)*. Renewable Energy, Underwriter's Laboratories; 2019:60062.
12. Voronko Y, Eder GC, Knausz M, Oreski G, Koch T, Berger KA. Correlation of the loss in photovoltaic module performance with the ageing behaviour of the backsheets used. *Prog Photovoltaics Res Appl*. 2015;23(11):1501-1515.
13. Kempe MD, Lockman T, Morse J. Development of Testing Methods to Predict Cracking in Photovoltaic Backsheets. In *2019 IEEE 46th Photovoltaic Specialists Conference (PVSC)*. IEEE; 2019:2411-2416.
14. Kempe MD, Lyu Y, Kim JH, Felder T, Gu X. Fragmentation of photovoltaic backsheets after accelerated weathering exposure. *Sol Energy Mater Sol Cells*. 2021;226:111044.
15. Gu X, Pan PC, Moffitt SL, et al. *Cracking and Microstructural changes of PVDF-Based Backsheets During Aging*. NREL Photovoltaic Reliability Workshop (PVRW); 2020.
16. Kempe MD, Lockman T, Morse J. *Development of Testing Methods to Predict Cracking in Photovoltaic Backsheets*. IEEE PVSC; 2019.

17. Meisel A, Mayer A, Beyene S, et al. SolarCity Photovoltaic Modules with 35 Year Useful Life. Solarcity and DNV-GL; 2016.
18. Doyle T, Erion-Lorico T, Desharnais R. *PV module reliability scorecard*. DNV-GL; 2018:1-32.
19. Gambogi WJ, Felder T, MacMaster S, et al. Sequential stress testing to predict photovoltaic module durability. *2018 IEEE 7th World Conference on Photovoltaic Energy Conversion (WCPEC) (A Joint Conference of 45th IEEE PVSC, 28th PVSEC & 34th EU PVSEC)*; IEEE; 2018.
20. IEC TS 63209-1 ED 1.0. *Extended-Stress Testing of Photovoltaic Modules—Part 1: Modules*. International Electrotechnical Commission; 2021:1-19.
21. IEC TS 63209-2 ED 1.0. *Extended-Stress Testing of Photovoltaic Modules—Part 2: Component Materials and Packaging*. International Electrotechnical Commission; 2022:1-13.
22. Kempe MD, Phillips NH. *Review of Modified Tensile Test Round Robin*. IEC TC 82 WG2 Presentation. Draft Publication in Progress. 2019. Michael.Kempe@NREL.gov
23. Lin CC, Lyu Y, Jacobs DS, et al. A novel test method for quantifying cracking propensity of photovoltaic backsheets after ultraviolet exposure. *Prog Photovoltaics Res Appl*. 2019; 27(1):44-54.
24. Kempe MD, Miller DC, Zielnik A, Montiel-Chicharro D, Zhu J, Gottschalg R. Survey of mechanical durability of PV backsheets. *2017 IEEE 44th Photovoltaic Specialist Conference (PVSC) (3208–3213)*, IEEE; 2017.
25. Felder TC, Gambogi WJ, Phillips NH, MacMaster SW, Yu BL, Trout TJ. Comparison of higher irradiance and black panel temperature UV backsheet exposures to field performance. In: Dhere NG, Sakurai K, Kempe MD, eds. *Reliability of Photovoltaic Cells, Modules, Components, and Systems X*. International Society for Optics and Photonics; 2017.
26. Yang S, Whitfield K, Rhee E. *UV Degradation Study of Encapsulate Backsheet System for PV Modules Using Metal Halide Lamp*. NREL PV Module Reliability Workshop; 2014.
27. Umamaheswari S, Murali M. FTIR spectroscopic study of fungal degradation of poly (ethylene terephthalate) and polystyrene foam. *Chem Eng*. 2013;64:19159-19164.
28. Sammon C, Yarwood J, Everall N. An FT-IR study of the effect of hydrolytic degradation on the structure of thin PET films. *Polym Degrad Stab*. 2000;67(1):149-158.

How to cite this article: Xia J, Liu Y, Hu H, et al. Impact of specimen preparation method on photovoltaic backsheet degradation during accelerated aging test. *Energy Sci Eng*. 2022;10: 1961-1971. doi:10.1002/ese3.1153